Molecular mechanical and quantum chemical study on the species involved in the hydrolysis of *cis*-diamminedichloroplatinum(II) and substituted bis(ethylenediamine)dichloroplatinum(II) complexes Part I. Reactants and products

G.St. Nikolov* and N. Trendafilova
Institute of General and Inorganic Chemistry, Bulgarian Academy of Sciences, Sofia 1113 (Bulgaria)

H. Schönenberger and R. Gust
Institute of Pharmacy, University of Regensburg, 8400 Regensburg (Germany)

J. Kritzenberger and H. Yersin
Institute of Physical and Theoretical Chemistry, University of Regensburg, 8400 Regensburg (Germany)

(Received July 27, 1993, revised November 17, 1993)

Abstract

Cisplatin and its substituted ethylenediamine derivatives, *cis*-$PtCl_2(R_2en)$ (en = ethylenediamine, R = H, Ph (phenyl), 2-, 3- and 4-PhOH) have been studied with respect to the first step of their hydrolysis reaction. The geometry of the reactants and products was determined by molecular mechanics (MM). The MM optimized structures were used to calculate by the extended Huckel method the charge distribution and relative electronic energies. The MM and EH calculations were carried out with different ligand conformations. Due to increased non-bonded repulsion, with increasing ligand bulkiness, the square planar arrangement is the preferred geometry also by the MM results. This additional (to the electronic) stabilization of the square planar arrangement around Pt(II) is unfavorable for the aquation process. The thermodynamic stabilities correlate with the rate of hydrolysis of *meso*-, (+)- and (−)-[1,2-bis(2-hydroxyphenyl)ethylenediamine]dichloroplatinum(II) (3-$PtCl_2$). The slower rate of hydrolysis of the *meso* diastereoisomer as compared with that of the *d, l* species of 3-$PtCl_2$ is explained by the presence of a 5th Pt–O contact in the *meso* diastereoisomer which hinders the entrance of the water molecule and makes the hydrolysis slower.

Key words: Quantum mechanical study; Platinum complexes; Ammine complexes; Halide complexes

Introduction

cis-$Pt(NH_3)_2Co_2$ (cisplatin) was the first platinum compound tested on a wide scale for cytostatic effects [1]. Since then the search for better and more potent compounds has been enlarged mainly by complicating the ligands. At present the Pt(II) coordination compounds are probably the most important reagents to attack DNA and cause antitumor effects [2]. Cross inhibition of DNA synthesis and subsequent cell death is believed to be the major mechanism. The presence of two easily dissociable groups (i.e. Cl^-) is essential for the cytostatic effect. The compounds, in which the two NH_3 are replaced by ethylenediamine and its derivatives also show a cytostatic effect [3]. The stereoisomers of the complexes 3-$PtCl_2$, 4-$PtCl_2$ and 5-$PtCl_2$ (Fig. 1) were tested against human breast cancer cell line as a tumor model [4–7]. Cisplatin is known [1] to bind to nucleobases after hydrolysis of the Pt–Cl bonds. The hydrolytic process of cisplatin is the rate determining step of the reaction of the antitumor compounds with DNA. The first step is:

$$cis\text{-}[Pt(NH_3)_2Cl_2] + H_2O \underset{k_{-1}}{\overset{k_1}{\rightleftharpoons}} [Pt(NH_3)_2(H_2O)ClCl]^{\#} \quad (a)$$

$$[Pt(NH_3)_2(H_2O)ClCl]^{\#} \rightleftharpoons cis\text{-}[Pt(NH_3)_2(H_2O)Cl]^+ + Cl^- \quad (b)$$

*Author to whom correspondence should be addressed.

SSDI 0020-1693(93)03765-3

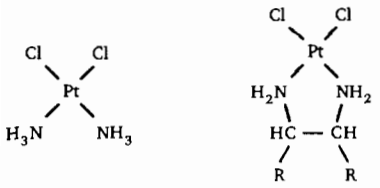

(a)

(b)

R	Compound
	1-$PtCl_2$
H	*meso*-, *d*, *l*-2-$PtCl_2$
Ph	*meso*-, *d*, *l*-3-$PtCl_2$
2-OH-Ph	*meso*-, *d*, *l*-4-$PtCl_2$
3-OH-Ph	*meso*-, *d*, *l*-5-$PtCl_2$
4-OH-Ph	

Fig. 1. Structural diagrams of cisplatin (a) and related compounds (b).

The half-life of formation of the mono aquo complex of *cis*-$Pt(NH_3)_2Cl_2$ was found to be about 2 h (37 °C) [8]. The mono aquo product reacts with DNA in a very short time (6 min).

Aquation proceeds via an associative mechanism S_N2; the transition state is probably a trigonal bipyramid in which the leaving group (Cl^-) and entering water molecule occupy the equatorial positions [1]. The equatorial Pt–Cl bond is longer than the axial Pt–Cl bond, since the compressed trigonal bipyramidal structure is preferred for the transition metal ML_5 compounds. This explains why Cl^- should leave from an equatorial rather than axial position.

The formation of the transition state complex (eqn. (a)), constitutes the first step in the hydrolytic reaction. This reaction is opposed by the high Cl^- concentration in the blood where the reverse reaction forming the dichloro complex cannot be excluded. However, in blood plasma pH = 7.4, $[Cl^-] = 0.103$ M, in the cell interior pH = 7.4, $[Cl^-] = 0.004$ M and near the nucleus $[Cl^-] = 0.15$ M [2]. Hence, after penetrating the cell, due to the lower Cl^- concentration in the cell interior, the hydrolysis of cisplatin is favored.

The rate of an irreversible reaction is governed by the energy barrier existing between reactants and products. However, the equilibrium position of a reversible reaction depends on the energy difference between the reagents and the products. To calculate the energy difference in the studied reversible hydrolysis reaction, it is essential to know the structure of the reactants and products. The structures of the reactants are in some cases known from X-ray diffraction studies, but those of the transition state complexes and the products – mono aquo complexes – cannot be obtained experimentally since they exist for a very short time under very specific conditions inside the cell. The fate of the mono aquo complexes is to either react monofunctionally with DNA or to undergo further hydrolysis before attaching bifunctionally to the DNA units [9]. The process of *cis*-Pt linking to DNA nucleobases has been studied in detail by Hambley [10], using molecular mechanics techniques. However, the mechanistic aspects of the hydrolysis process preceding this linking are still not clear.

In the first part of this series we shall examine the geometric and electronic structures of the reactants and the products of a number of cisplatin compounds. The transition state structures are discussed in Part II of the series.

Two points must be discussed in advance in relation to the possible avenues of examination:

(i) Pt(II) (d^8 electron configuration) usually produces square planar complexes [11–14]. This preferencc is attributed to electronic factors – the unoccupied d-MO (LUMO) is much higher in energy than the highest occupied MO (HOMO) and the large HOMO–LUMO gap is responsible for the formation of square planar low-spin Pt(II) complexes. Several arguments have been voiced, however, against this oversimplistic explanation [12]. Besides the electronic factors, interligand repulsion (ILR) or non-bonded interactions, are very important [13] in shaping the geometry. The ILR energy for a four-coordinate complex is at a minimum for a tetrahedral arrangement of the ligands, which is in fact the highest symmetry ML_4 polyhedron. Distortion of the tetrahedral arrangement towards a square planar one for metal d^8 complexes is connected with an increase in ILR energy (destabilization), which in this particular case of d^8 is compensated by a decrease in electronic energy (stabilization) [14]. The final geometric structure should be a compromise between the two factors.

In four-coordinate Pt(II) compounds the electronic factor seems to dominate: in all the known crystal structures Pt(II) forms square planar species [15–21]. However, a conversion towards a tetrahedral structure would favour an S_N2 substitution mechanism since the d^8 ML_4 tetrahedral species are kinetically labile and the stereochemical isomers lose their identity rather quickly [14]. The conversion would depend on the energy difference (Δ) between the two structures. The Δ value is high for d^8 ML_4 with simple (e.g. monoatomic) ligands. However, with bulky ligands the ILR energy component increases while the electronic factor remains almost constant if the donor atoms set is the same; in this case the tetrahedral structure may approach in energy the planar one. Hence it is interesting to get a glimpse of the square planar–tetrahedral energy difference; the tetrahedral structure is hypothetical and accessible only theoretically.

For this reason we have studied both the square planar and the hypothetical tetrahedral structures for the reactants and products. Moreover, the tetrahedral aquation products may offer better chances to bind to

single stranded nucleic acids or to cross link double stranded DNA.

(ii) The studied organic ligands may exist in several conformations prior to coordination. Upon coordination, some of the conformers become inaccessible due to steric reasons. However, others may be retained. It is essential to assess the relative conformational stability of the reactants and products, since we do not know in advance which conformer would provide the best chances for linking to DNA. If conformers of higher energy offer better conditions for such a linking, and if they are accessible by energy from the lowest energy conformer, then one should be interested in learning more about their structure and stability. This is especially relevant for the substituted ethylenediamine (en) complexes examined here. For this reasons we examine both the stable symmetric (gauche, also called envelope structure) and unstable asymmetric (chair, also called half-chair structure) conformers of the en ligands see Fig. 2) as well as their *d*, *l* and *meso* isomers (see Fig. 3).

The complexes examined as reactants of the aquation process in this work are *cis*-Pt(L-L)Cl_2, where L-L= $2NH_3$

H_2N–CH_2–CH_2–NH_2	(en)
H_2N–CHPh–CHPh–NH_2	(Ph–en–Ph)
H_2N–CH(2-OHPh)–CH(2-OHPh)–NH_2	(2-OHPh–en–2-OHPh)
H_2N–CH(3-OHPh)–CH(3-OHPh)–NH_2	(3-OHPh–en–3-OHPh)
H_2N–CH(4-OHPh)–CH(4-OHPh)–NH_2	(4-OHPh–en–4-OHPh)

(1)

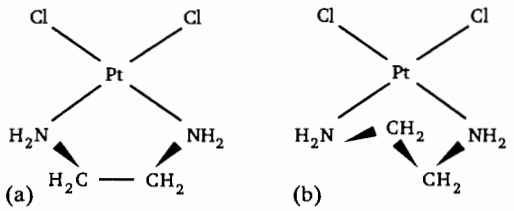

Fig. 2. Chair (a) and gauche (b) conformers of the en ligand in Pt(en)Cl_2.

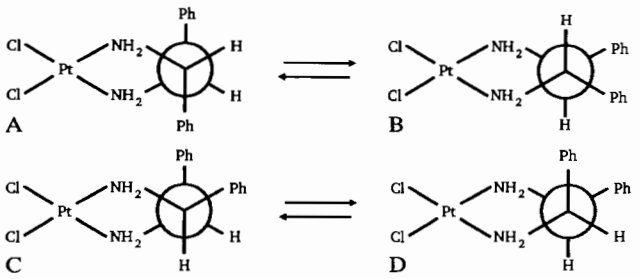

Fig. 3. Possible conformers of stereo isomeric forms of 2-, 3-, 4- and 5-$PtCl_2$ [4]: A, ¦*d*, *l*; B, >*d*, *l*; C and D, *meso*.

The ligands are ordered so as to reflect the ligand complexity. This series was chosen since the cytostatic effect of the separate complexes has been reported previously [6, 7]. Figure 3 illustrates the possible conformers >*d*, *l* (both Ph in equatorial position) (B), ¦*d*, *l* (both Ph are in axial position (A) and two *meso* (one Ph is in equatorial, the second in axial position) (C, D).

The crystal structures of some of these compounds are already known [15–20]. However, the structures in solution may differ. Moreover, if some molecular structures were taken from X-ray studies and others from geometry optimization, a comparison between them would be unrealistic. To make possible the comparison between the different compounds we have treated them all by molecular mechanics. To assess the reliability of the results the geometries obtained are compared with those from X-ray determinations but minor differences are ignored. The MM optimized geometries were used to calculate the electronic structures by the extended Hückel method.

Extensive electronic structure calculations have also been carried out for some of the complexes described above [22–26]. They involve *ab initio* [22], relativistic EH [23], INDO [24, 25] and Xα [26] calculations. However, the calculations refer to a limited number of complexes with ligands from our list and they cannot be used in the comparative study we have in mind. For this reason all compounds were treated in the same way by the EH method. The results thus obtained were compared with those from the literature in the cases where it was possible (only for *cis*-$Pt(NH_3)_2Cl_2$ and *cis*-$Pt(NH_3)_2Cl(H_2O)^+$).

Theoretical

We have used the standard MMX (enhanced version of MMP2) procedure with the parameters collected in its 1988 version [27]. Since the enthalpy increments for the Pt–N, Pt–Cl and Pt–O bonds are not included in this version, the calculated ΔH_f (enthalpy of formation) are meaningless unless compared for similarly constituted compounds. The MM energy or the closely matching strain energy (SE) provide the best quantity to access the relative stability of the compounds [10].

In some cases, especially for cisplatin and its unsubstituted en derivative, MM calculations, which ignore explicitly the electronic factors, gave lower energies for the tetrahedral structures as compared with the planar. In other cases, however (*vide infra*), the MM calculations pointed to the planar structure to be lower in energy than the tetrahedral; the reason is the increased re-

pulsion between the remote part of the ligand and/or the approach of the ligand's atoms to the axial positions of the square planar compound, which behaves as five- or six-coordinate species. To calculate the geometry of the higher energy structure (square planar or tetrahedral) by the MM method we fixed the donor atoms in the *xy* plane for the planar structure when the tetrahedral was the more stable one, or with respect to the C_3 axis for the tetrahedral structure, when the square planar was more stable. For the square planar compounds this fixing takes into account the electronic factor explicitly. For the tetrahedral species, the fixing of distances reflects the desire to obtain a higher energy structure and prevents the molecule collapsing into the lowest energy geometry. The problem concerning the treatment of the square planar structure was also present in Hambley's [11] studies. He resolved it in another way by locating two dummy H atoms normal to the molecular plane in order to keep the molecule planar. We believe our treatment is more realistic.

The extended Hückel calculations were performed using a version [28] which uses a metal–ligand distance-dependent formula to calculate the off-diagonal elements. Charge iteration was performed in all cases. The atomic parameters were taken basically from the collections of Fitzpatrick and Murphy [29] and Calzaferri *et al.* [28] but the Pt orbital exponent had to be readjusted to a Slater-type orbital (STO) to obtain a slightly positive Pt charge in the complex; with Fitzpatrick's parameters q(Pt) was always negative. The Pt valence state ionization potentials (VSIP) were taken from ref. 30 (see Appendix). Three different energies are obtained by the EH method: sum of orbital energies, orbital stabilization energy and repulsion energy. In order to facilitate comparison between differently constituted complexes we use the orbital stabilization energy which is defined as the difference between the sum of energies for the orbitals populated with electrons and the respective VSIP (see ref. 28).

The computational procedure adopted here is as follows. We have calculated the geometry of the compounds by the MMX [27]. Then the MM-produced geometry is used as input to calculate the electronic structure by the EH method. The results obtained (metal charge, bond orders, electrostatic potential etc.) are used to discuss possible correlations between molecular structure and electronic structure as well as with biological activity. Such correlations have already been established [31, 32a].

To assess the reproducibility of the results, we have performed the MM calculations for a given complex several times, starting each time with a molecule drawn in a different way. The MM energy components were reproduced within ± 0.1 kJ mol^{-1}. The EH calculations gave the energies with ± 0.01 eV or lower and the charges differed by less than 0.02 units.

Results and discussion

Reactants

The results are collected in Table 1. We shall first discuss them separately for the different compounds and then in a comparative way. The notations are explained in Fig. 1.

cis-Pt(NH$_3$)$_2$Cl$_2$. It is readily seen that the molecular structure reported by X-ray diffraction [16, 34] is in agreement with the one obtained from MM calculations: (a) the calculated bond lengths are longer by 0.1 Å than the experimental but the order Pt–Cl > Pt–N is correct; (b) the calculated valence angles are correct within $\pm 2°$. The MM results are better (compared to the experiment) than those from *ab initio* calculations [22] as regards the valence angles and worse as regards the bond lengths. It should be noted that for this compound the planar structure was obtained only when the ligand donor atoms were fixed in the molecular plane. Set free (atoms not fixed), the structure collapses to a tetrahedral one with an MM energy gain of ~ 7 kJ mol^{-1}. As expected for d^8, the EH results, however, gave a definite preference for the planar structure: the electronic energy gain from EH calculations upon distorting the tetrahedral complex to planar is about 318 kJ mol^{-1} much greater than the ILR energy gain for the reverse process -7 kJ mol^{-1}. The calculated charges are q(Pt) = 0.066, q(Cl) = -0.465.

Our EH results on *cis-* and *trans*-Pt(NH$_3$)$_2$Cl$_2$ show that the *cis* form is more stable. It should be noted however that the MM results point to a different picture: the *trans* form is more stable in terms of repulsion between the two NH$_3$ groups – the repulsion is greater in the *cis* form than in the *trans* form. This is in agreement with CNDO [25a], INDO [24] and *ab initio* [22] calculations. An interesting result also came from MM calculations: the *cis* form when the donor set atoms were not fixed converts to tetrahedral; the *trans* form needs no fixing of the atoms' positions – it remains planar in both cases. This picture is fully consistent with the increased NH$_3$–NH$_3$ repulsion in the tetrahedral species as compared with the *trans* planar isomer.

1-PtCl$_2$. The planar structure was obtained only when the donor atoms were fixed in the molecular plane. For this compound the en ligand can assume a symmetric (gauche) or asymmetric (chair) conformation (see Fig. 2). It is readily seen (Table 1) that MM predicts the *cis*-Pt(en)Cl$_2$ complex with gauche en conformation to be more stable than the complex with chair en. The energy difference between gauche and chair conformers is -25.1 kJ mol^{-1} in favour of the gauche form. The

TABLE 1. Energy data (EH[a] and MM[a]) and charge distribution for the reactants

cis-$Pt(NH_3)_2Cl_2$	Calc.	Exp. [16]	Exp. [34]	Calc. [22] *ab initio*
EH (kJ mol^{-1})	−4521.2			
q(Pt)	0.066			
q(Cl)	−0.465			
LUMO–HOMO (kJ mol^{-1})	404.9			
MM (kJ mol^{-1})				
(planar − fixed)	7.9			
Pt–Cl (Å)	2.43	2.33	2.33	2.29
Pt–N (Å)	2.11	2.01	2.01	2.08
Cl–Pt–Cl (°)	93 2	92.0	92.0	95.8
N–Pt–N (°)	87.2	87.0	87.0	96.4
N–Pt–Cl (°)	89.1	88.5	90.5	83.9
	90.4	92.0	90.5	83.9

1-$PtCl_2$ {$Pt(en)Cl_2$}	Calc.		Exp. [15]
	Chair	Gauche	Gauche
EH (kJ mol^{-1})	−8454.3	−8473.6	
q(Pt)	0.115	0.062	
q(Cl)	−0.545	−0.467	
LUMO–HOMO (kJ mol^{-1})	356.7	385.6	
MM (kJ mol^{-1})			
(planar − fixed)	36.8	11.7	
Pt–Cl (Å)	2.43	2 24	2.29
Pt–N (Å)	2.13	2.12	2.08
Cl–Pt–Cl (°)	100.5	97 0	96.4
N–Pt–N (°)	69.5	80 5	73.0
N–Pt–Cl (°)	94.1	91.2	95.3
	95.9	91.2	95.3

2-$PtCl_2$ {Pt(Ph–en–Ph)Cl_2}	Chair	> *d, l* (B)[b]	*meso* (C=D)[b]	¦*d, l* (A)[b,c]
EH (kJ mol^{-1})	−24668.8	−24711 2	−24663.9	−24638.9
q(Pt)	0.110	0.112	0.120	0.124
q(Cl)	−0.555	−0.550	−0 545	−0.543
LUMO–HOMO (kJ mol^{-1})	366.3	383.7	391.4	393.8
MM (kJ mol^{-1})				
(planar − fixed)	120.5	85.4	86.6	75.3
Pt–Cl (Å)	2.43	2.43	2.43	2.43
Pt–N (Å)	2.12	2.12	2.12	2.12
Cl–Pt–Cl (°)	100.5	97.4	97.6	97.3
N–Pt–N (°)	70.1	80.2	80.4	80.5
N–Pt–Cl (°)	94.7	91.5	91.7	91.2
	94.7	91.5	90.7	90.9

3-$PtCl_2$ {Pt(2-OHPh–en–2-OHPh)Cl_2}	Chair	> *d, l* (B)[b] Calc.	Exp. (B) [34]	*meso* (C=D)[b] Calc.	Exp. (C=D) [34]	¦*d, l* (A)[b,c] Calc.
EH (kJ mol^{-1})	−25565.3	−25626.9		−25479.9		−25288.6
q(Pt)	0.116	0.116		0.095		0.104
q(Cl)	−0.516	−0.548		−0.560		−0.567
LUMO–HOMO (kJ mol^{-1})	337.4	369.4		356.4		230.2

(continued)

TABLE 1. (*continued*)

3-$PtCl_2$ {Pt(2-OHPh–en–2-OHPh)Cl_2}	Chair	$>d,l$ (B)[b] Calc.	Exp. (B) [34]	*meso* (C=D)[b] Calc.	Exp. (C=D) [34]	$\|d,l$ (A)[b,c] Calc
MM (kJ mol^{-1})						
(planar – fixed)	113.0	77.8		84.5		73.2
Pt–Cl (Å)	2 44	2.44	2.30	2.44	2.31	2.44
Pt–N (Å)	2.12	2.12	2.08	2.12	2 07	2.12
Cl–Pt–Cl (°)	101.1	97 7	94.8	97.9	92.4	96.2
N–Pt–N (°)	72.3	80.7	83.0	80.1	81 2	80.2
N–Pt–Cl (°)	93.0	91.7	90.1	91.0	93 3	91.6
	94.6	92.0	92.1	91.0	93.3	92.0
Pt–OH (Å)				2.22	2.40	

[a]EH = orbital stabilization energies; MM = molecular mechanical energies. [b]Gauche forms. [c]Never observed experimentally.

same prediction comes up from the electronic energy; there is a net gain of 19.3 kJ mol^{-1} on going from the chair to the gauche form. This finding is in agreement with the experimental X-ray diffraction data, which show that the C–C bond is slanted to the PtN_2Cl_2 plane, one C atom above and the other below (gauche conformer) [15]. The experimental and calculated (for the gauche form) values of the bond distance and valence angles compared well (±0.05 Å, ±1 to 7°).

It should be noted that the compound with the chair form offers a longer Pt–Cl bond and a larger Cl–Pt–Cl angle (see Table 1). The most sensitive parameter upon the chair–gauche conformer conversion is the N–Pt–N angle; it is the same in the diammine and the gauche en complexes (*c.* 80°) but drops to 70° when the chair conformation is realized; this change is accompanied by the opening of the Cl–Pt–Cl angle. Hence a gauche–chair conformer conversion in the solution is possible and it may readjust the direction of the Pt AOs which is essential in the Pt–Cl cleavage.

The EH energy difference between the planar gauche and a tetrahedral gauche form is −298.8 kJ mol^{-1} in favor of the planar form. The loss of MM energy on going from the tetrahedral to planar form is small ~5.0 kJ mol^{-1}. This finding, compared with the big difference between the MM energy for the *cis*-$Pt(NH_3)_2Cl_2$ complex suggests that en produces more ILR in the tetrahedral form than two NH_3 and thus substitution of two NH_3 with an en would contribute to shaping a planar compound.

2-$PtCl_2$. The same conclusions about gauche and chair conformers can be reached when two phenyl groups are introduced in 1,2-positions in the en ligand. Both MM and EH favor the gauche conformer ($>d,l$). EH energy difference planar–tetrahedral is the same as for 1-$PtCl_2$ (−298.8 kJ mol^{-1} in favor of the gauche planar), but the planar gauche ($>d,l$)–chair energy difference is −42.4 kJ mol^{-1} – twice the amount with unsubstituted en. Hence, the gauche–chair energy difference is higher for 2-$PtCl_2$ as compared with 1-$PtCl_2$ and the compound should have a gauche Ph–en–Ph conformer also in solution. An analysis of the resulting MOs (EH calculations) has shown that the Ph MOs are well separated by energy from the MOs of the rest of the system. The substitution of en by Ph–en–Ph retains the gauche form and the planar arrangement. It should be noted that the planar structure of the *meso* and the $|d,l$ forms with axial phenyl groups (see Fig. 3) was obtained even in the case when the ligand donor atoms were *not* fixed in a plane. Only the $>d,l$ form with equatorial phenyl groups showed a slight deviation from the planar structure. Obviously, the increased bulkiness of the ligand increases the ILR energy, and the planar structure which offers better conditions for the en substituents becomes stabilized even in terms of the MM energy. The substituents may block access to the 5th and 6th axial positions of the square planar compound which kinetically would behave as octahedral rather than square planar. Similar results were obtained with other square planar complexes [32b].

3-$PtCl_2$. The substitution of en by PhOH–en–PhOH (3-$PtCl_2$) also retains the planar structure and the gauche form in the MM calculations. Here again the ligand donor atoms need not be fixed in a plane to obtain a planar structure for the *meso* and the $|d,l$ forms with axial phenyl groups. This finding was explained in terms of the ILR factor (*vide supra*). The gauche ($>d,l$) form is more stable by 61.6 kJ mol^{-1} (EH) and 35.2 kJ mol^{-1} (MM) than the chair form.

Comparison between the different Pt(II) complexes

Before attempting to diversify the hydroxy phenyl derivatives as to the possible optical isomers, some insight into the nature of the reactants may be gained by comparing the parameters obtained for the complexes with en ligands and its derivatives. With respect to the gauche–chair energy difference (for 2- and 3-$PtCl_2$–gauche ($>d,l$)–chair) both EH and MM results

predict the order:

$$1\text{-}PtCl_2 < 2\text{-}PtCl_2 < 3\text{-}PtCl_2 \quad (2)$$

In this order the difference increases from left to right, i.e. the gauche form is stabilized with increasing ligand bulkiness. The planar–tetrahedral energy difference is (both gauche; for 2- and 3-$PtCl_2$ gauche ($>d,l$)):

$$\text{cisplatin} > 1\text{-}PtCl_2 \sim 2\text{-}PtCl_2 > 3\text{-}PtCl_2 \quad (3)$$

Setting aside the cisplatin complex, gauche-planar en complexes may convert to gauche-tetrahedral with almost no change in MM and electronic energy.

In the studied ligand series the hydroxy phenyl derivative produces the highest positive charge on Pt, calculated by the EH method. The chair forms produce higher q(Pt) than the gauche forms only for the en ligand. In the phenyl and hydroxy phenyl complexes the gauche and chair forms have equal charge on Pt.

The charges on the chloride ions, q(Cl) are:

$$\text{cisplatin} \sim 1\text{-}PtCl_2 < 2\text{-}PtCl_2 \sim 3\text{-}PtCl_2 \text{ for gauche} \quad (4)$$

$$1\text{-}PtCl_2 \sim 2\text{-}PtCl_2 > 3\text{-}PtCl_2 \text{ for chair} \quad (5)$$

The chair forms produce more negative q(Cl) than the gauche forms of the en and the phenyl ligands. It can be expected that the release of one Cl in the hydrolysis reaction would be connected with a flow of electrons towards Cl to form Cl^-. Another factor that may favor this reaction is the high positive charge on Pt. This case – high positive Pt and high negative Cl^- would correspond to an electrostatic Pt–Cl bond being formed with electron redistribution – as the first step in Pt–Cl bond rupture. An inspection of the results obtained show that the hydroxy phenyl gauche $>d,l$ derivative gives high positive q(Pt) and high negative q(Cl). Since the gauche $>d,l$ form of the hydroxy phenyl complex (3-$PtCl_2$) is most easily hydrolyzed it may be concluded that the expectations as to charge redistribution are best satisfied by this compound (see Table 1).

The trend as to the gauche-chair LUMO–HOMO difference is for gauche:

$$\text{cisplatin} > 1\text{-}PtCl_2 \sim 2\text{-}PtCl_2 > 3\text{-}PtCl_2 \quad (6)$$

Diastereomeric complexes of the substituted en complexes

The two possible diastereomeric complexes of the compounds with Ph groups (d,l and *meso*) (see Fig. 3) will be considered. It was not possible to distinguish between the optical isomers $d(+)$ and $l(-)$ forms (insignificant MM energy difference). Thus, we shall consider further $d(+)$ and $l(-)$ together as a d,l form. Since MM calculations have already shown a definite preference to the gauche conformer of the en ligand as compared with the chair conformer only the first one will be dealt with. The reactants were treated first as isolated molecules which are not influenced by the solution environment. A model for the species in solution is also considered further. In both steps four conformers are dealt with (see Fig. 3). The results from MM calculations with the d,l (A and B), (gauche) and *meso* (gauche) forms of 2-$PtCl_2$ compound show that the two *meso* forms do not differ significantly in MM energy (C ≈ D). However, the *meso* forms are unstable as compared with the d,l forms of which the $\dot{|}d,l$ (A) form with Ph groups in axial positions is the most stable one. The MM energy difference between (B) and (A) forms is 10.1 kJ mol^{-1} in favour of the (A) form (Table 1). The lower MM energy for the $\dot{|}d,l$ (A) form can be explained by lower Ph–Ph repulsion as compared with the repulsion in the other $>d,l$ form. The $|d,l$ form was never observed experimentally.

In order to simulate the environment of the complex in solution a model was considered in which two water molecules are associated to platinum – above and below the N–Pt–N plane. The results obtained with this model show definitely that the $\dot{|}d,l$ conformer with both Ph groups in axial position (A) has higher energy ($\Delta = 12.6$ kJ mol^{-1}) as compared with the $>d,l$ form with Ph groups in equatorial positions (B). This finding is strongly supported by the fact that the (A) form is never observed experimentally [33, 34].

The EH results show the same trends as to the stability of the studied forms: the EH energy difference (B)–(A) is in favour of (B). The *meso* forms show higher EH energy than the $>d,l$ form (see Table 1).

A new interesting trend emerges when the d,l and *meso* diastereomers of 3-$PtCl_2$ are compared. The two *meso* forms are higher in MM energy as compared with the d,l forms (Table 1). For the 2-$PtCl_2$ compound the *meso* (C, D) and $>d,l$ forms with equatorial Ph groups (B) do not differ significantly in MM energy ($\Delta = 1.2$ kJ mol^{-1}). The (B) $>d,l$ form of 3-$PtCl_2$ is of lower energy by 6.7 kJ mol^{-1} than the *meso* forms (see Table 2). The EH results give definitely preference to the (B) form since it has the lowest EH energy.

X-ray crystallographic data for $>d,l$ and *meso* forms (Table 1) have shown small differences between the calculated and experimental bond angles and bond lengths of the PtN_2Cl_2 unit of 3-$PtCl_2$ [34]. Two different $>d,l$ molecules were found in the solid state. A comparison between the experimental data for the $>d,l$ and the *meso* forms shows that the Pt–Cl and Pt–N bond lengths are equal within experimental error. However, differences between these two forms have been observed for the Cl–Pt–Cl, N–Pt–N and N–Pt–Cl angles: the Cl–Pt–Cl angle is larger in the $>d,l$ form (94.8°) as compared with the *meso* form (92.4°), the same holds also for the N–Pt–N angle (83.0 and 81.2°, respectively).

Conversely, the two N–Pt–Cl angles are smaller for the $>d,l$ form (90.1, 92.1°) as compared with those for the *meso* form (93.3, 93.3°). The calculated angles follow the trends of the experimental data with the exception of the N–Pt–Cl angles – they were not very different for the d,l and *meso* forms.

In the MM produced structure the *meso* form of 3-$PtCl_2$ shows five-coordinate Pt(II) through a Pt–O contact (2.22 Å). The oxygen atom of the phenyl group, which is nearly perpendicular to the best PtN_2Cl_2 plane, is over the Pt atom. Using the available X-ray data [34] for the *meso* form of the 3-$PtCl_2$ compound, rotation around the phenyl–en bond yields a minimal Pt–O distance of 2.4 Å. Such a rotation is possible in solution. The two distances compare well.

Comparison with biologic activity

It is interesting to compare the results for 3-$PtCl_2$ (OH in 2-position), with those for the same compound but with OH in 3- and 4-positions of the Ph groups (compounds 4-$PtCl_2$ and 5-$PtCl_2$) (see Table 2 and Fig. 1).

Recent studies have shown that the hydroxy phenyl complexes with OH in 3- and 4-position in the phenyl rings are potent with respect to the Ehrlich ascites mouse tumor [33]. However, only the 3-hydroxy phenyl derivatives led to an inhibition of the cisplatin-resistant tumor growth. It was further found that the shift of both OH groups from 3- into 2-position (compound 3-$PtCl_2$) produces a distinct elevation of the antitumor activity on the cisplatin-resistant Ehrlich ascites tumor. A comparison of the MM energy for the complexes without OH and with OH in 2-, 3- and 4-position is given in Table 2. The results show that only in the case of the 3-$PtCl_2$ compound do both *meso* forms have significantly higher MM energy as compared with the $>d,l$ form ($\Delta = 6.7$ kJ mol^{-1}). Insignificant energy differences between the *meso* and $>d,l$ forms with equatorial Ph groups were found for the compounds without OH ($\Delta = 1.2$ kJ mol^{-1}) and with OH in 3- ($\Delta = 2.2$ kJ mol^{-1}) and 4- ($\Delta = 2.3$ kJ mol^{-1}) positions. Obviously, the OH groups in 2-position of the phenyl ring stabilize the $>d,l$ form of the 3-$PtCl_2$ compound with a significantly lower energy as compared with the *meso* form. At the same time, the $>d,l$ form of the 3-$PtCl_2$ compound showed a more rapid hydrolysis process than the *meso* form. It is difficult to explain why the more stable form of the 3-$PtCl_2$ compound was easier to hydrolyze and showed higher antitumor activity. Two factors can provide a possible explanation: (i) the position of the OH groups in the phenyl ring and (ii) the orientation of the phenyl rings with respect to the PtN_2Cl_2 plane. When OH are in second position of the phenyl rings and when these phenyl rings are in equatorial orientation ($>d,l$ isomer of 3-$PtCl_2$), they do not interfere with the entering H_2O molecule and the Pt environment is the most suitable one.

The slower hydrolysis observed for the *meso* isomer of the 3-$PtCl_2$ compound as compared with that of the $>d,l$ isomer could be explained by the presence of the 5th Pt–O contact (between one OH group and Pt atom) which is short (2.22 Å) and oriented nearly perpendicular to the best PtN_2Cl_2 plane: it thus prevents the entrance of the water molecule. In the $>d,l$ isomer of the same compound the phenyl substituents with OH groups are in equatorial positions and such contacts are not possible. This fact facilitates the entrance of the water molecule over and below the PtN_2Cl_2 plane. The stabilizing OH effect is smaller for the 3- and 4-hydroxy phenyl (compounds 4-$PtCl_2$ and 5-$PtCl_2$) (OH groups are far enough away from the Pt atom) as well as for the compound without OH (compound 2-$PtCl_2$). This is in agreement with our EH results which have shown that with the OH in 2-position the PhOH MOs intervene heavily with the MOs of the rest of the system but this was not the case for the 2-$PtCl_2$ where the Ph MOs are well separated. Obviously, the second position of the OH is the most suitable one but only when the phenyl rings are in equatorial location.

The MM energy differences for the different diastereoisomers are small (1–7 kJ mol^{-1} for the $>d,l$–*meso*) and rapid interconversion may occur. The higher rate of hydrolysis for the d,l form will be further examined in Part II of this series.

TABLE 2. MM[a] and SE[a] energy (kJ mol^{-1}) for the reactants 2-, 3-, 4- and 5-$PtCl_2$

Reactants		$>d,l$[b] (B)	*meso*[b] (C=D)	$\{d,l$[b,c] (A)
2-$PtCl_2$	MM	85.4	86.6	75.3
{Pt(Ph–en–Ph)Cl_2}	SE	82.6	84.0	72.6
3-$PtCl_2$	MM	77.8	84.5	73.2
{Pt(2-OHPh–en–2-OHPh)Cl_2}	SE	75.2	82.1	70 7
4-$PtCl_2$	MM	80.5	82.7	70.6
{Pt(3-OHPh–en–3-OHPh)Cl_2}	SE	77.7	79.9	67.8
5-$PtCl_2$	MM	79.8	82.1	69.7
{Pt(4-OHPh–en–4-OHPh)Cl_2}	SE	77.1	79.4	66 9

[a]MM = molecular mechanical energy, SE = strain energy. [b]Gauche forms. [c]Never observed experimentally.

Hydrolysis products

MM and extended Hückel calculations were performed for the hydrolysis product of the reactants listed above. The results are compared in Table 3. Both gauche and chair conformers of the en ligand were considered.

TABLE 3. Energy data (EH[a] and MM[a]) and atomic charge distribution for the hydrolysis products

$[Pt(NH_3)_2(H_2O)Cl]^+$				
EH (kJ mol^{-1})	−5870.8			
q(Pt)	0.103			
q(Cl)	−0.445			
LUMO–HOMO (kJ mol^{-1})	443.4			
MM (kJ mol^{-1})	40.3			
Pt–Cl (Å)	2.24			
Pt–O (Å)	1.86			
Pt–N (Å)	2.11			
1-Pt(H_2O)Cl $[Pt(en)(H_2O)Cl]^+$	Chair	Gauche		
EH (kJ mol^{-1})	−8454.3	−8724.2		
q(Pt)	0.109	0.140		
q(Cl)	−0.561	−0.529		
LUMO–HOMO (kJ mol^{-1})	134.9	395.2		
MM (kJ mol^{-1})	59.4	34.7		
Pt–Cl (Å)	2.44	2.43		
Pt–O (Å)	1.95	1 96		
Pt–N (Å)	2 13	2.12		
2-Pt(H_2O)Cl $[Pt(Ph\text{–}en\text{–}Ph)(H_2O)Cl]^+$	Chair	$>d,l$[b] (B)	*meso*[b] (C=D)	$_{\|}^{\|}d,l$[b,c] (A)
EH (kJ mol^{-1})	−24929.0	−24962.8	−24919.4	−24880.8
q(Pt)	0.133	0.132	0.140	0.143
q(Cl)	−0.542	−0.542	−0.538	−0.534
LUMO–HOMO (kJ mol^{-1})	375 9	401 9	411.7	387.3
MM (kJ mol^{-1})	144.6	109.3	110.7	100.6
Pt–Cl (Å)	2.43	2.43	2.43	2.43
Pt–O (Å)	1.95	1.96	1.96	1.96
Pt–N (Å)	2.12	2 12	2.12	2.12
3-Pt(H_2O)Cl $[Pt(2\text{-}OHPh\text{–}en\text{–}2\text{-}OHPh)(H_2O)Cl]^+$	Chair	$>d,l$[b] (B)	*meso*[b] (C=D)	$_{\|}^{\|}d,l$[b,c] (A)
EH (kJ mol^{-1})	−25719.5	−25864.1	−25719.5	−25574.9
q(Pt)	0.124	0.131	0.110	0.125
q(Cl)	−0.503	−0.541	−0 554	−0.556
LUMO–HOMO (kJ mol^{-1})	221.7	366.3	338 0	239.4
MM (kJ mol^{-1})	130.0	101.9	108.8	96.7
Pt–Cl (Å)	2.43	2.43	2.43	2.43
Pt–O (Å)	1.96	1.96	1.96	1.96
Pt–N (Å)	2.12	2.12	2.12	2.12

[a]EH = orbital stabilization energy; MM = molecular mechanical energies. [b]Gauche forms. [c]Never observed experimentally.

The MM and EH energies show that the gauche conformer is greatly preferred also in the products. The two phenyl rings in a chair conformation are rather close even in the hydrolysis product and this makes the chair conformer unfavorable.

In order to avoid traps in force-field local minima, the hydrolysis products were studied by MM in two different ways: (i) starting from the reactant structures and substituting one Cl by H_2O and (ii) starting from the possible transition state complexes with coordination number 5 and releasing one Cl^-. Both starting points give practically the same results. For 2-Pt(H_2O)Cl, both the *meso* and $>d,l$ forms with Ph groups in equatorial position (B) are of higher energy as compared with the other $_{\|}^{\|}d,l$ form (A).

The EH results for 2-Pt(H_2O)Cl show the most stable form to be the gauche $>d,l$ (B) form.

For the d,l and *meso* forms of 3-Pt(H_2O)Cl hydrolysis products both *meso* conformers have higher energy when compared with the d,l conformers but the difference is much higher when compared with the 2-$PtCl_2$ compound (see Table 4). The EH calculations for this compound again give a definite preference to the gauche $>d,l$ (B) (Table 3).

Similarly to the reactants, the hydrolysis products with bulky ligands (2-Pt(H_2O)Cl and 3-Pt(H_2O)Cl) ad-

TABLE 4. MM[a] and SE[a] energy for the hydrolysis products 2- and 3-$Pt(H_2O)Cl$

Hydrolysis products		>d,l[b] (B)	meso[b] (C=D)	¦d,l[b,c] (A)
MM and SE energy (kJ mol^{-1})				
2-$Pt(H_2O)Cl$	MM	109.3	110.7	100.6
{Pt(Ph-en-Ph)$(H_2O)Cl$}	SE	114 9	116.3	106.2
3-$Pt(H_2O)Cl$	MM	101.9	108.8	96 7
{Pt(2-OHPh-en-2-OHPh)$(H_2O)Cl$}	SE	107.5	114.4	102.3

[a]MM = molecular mechanical energy, SE = strain energy. [b]Gauche forms. [c]Never observed experimentally

TABLE 5. Differences between the EH and MM parameters of the products and reactants accompanying the hydrolysis reaction (in kJ mol^{-1})

Compound	EH			MM		
	ΔEH	Δq(Cl)	Δq(Pt)	ΔMM	ΔSE	ΔPt–Cl
cis-$Pt(NH_3)Cl$	−1349.6	0.020	0.040	32.40	35.31	−0.19
1-$PtCl_2$	−250.6	−0.06	0.080	23.00	31.42	0.19
2-PtCl >d,l	−251.6	0.008	0.020	23.90	32.30	0.00
2-$PtCl_2$ ¦d,l	−241.9	0.009	0.020	25.30	33.60	0.00
2-$PtCl_2$ *meso*	−255.5	0 007	0.020	24.10	32.30	0 00
3-$PtCl_2$ >d,l	−237.2	0 007	0.015	24.10	32.30	−0.01
3-$PtCl_2$ ¦d,l	−286 3	0.011	0.021	23.50	31.60	−0.01
3-$PtCl_2$ *meso*	−239.6	0.006	0.015	24.30	32 30	−0.01
4-$PtCl_2$ >d,l	−231.6	0.007	0.019	22.40	30.80	−0.01
4-$PtCl_2$ ¦d,l	−241.2	0.010	0.020	25.30	33.70	0.00
4-$PtCl_2$ *meso*	−212.3	0 013	0.025	24.10	32.40	0.00
5-$PtCl_2$ >d,l	−230 6	0.007	0.019	22.20	30.60	−0.01
5-$PtCl_2$ ¦d,l	−240.2	0.007	0.024	24 80	33.20	0.00
5-$PtCl_2$ *meso*	−221.9	0.009	0.021	23.90	32.30	0.00

For 1-, 2-, 3-, 4- and 5-$PtCl_2$ only gauche form is considered.

ditionally stabilize their *meso* and ¦d,l forms with the axial phenyl substituents in a planar arrangement. MM yields a nearly planar structure without fixing the donor atoms in a plane. The structure of the other >d,l form with equatorial phenyl groups, however, was planar only when the ligand donor atoms were fixed in a plane during the optimization procedure. This was the case also for *cis*-$Pt(NH_3)_2(H_2O)Cl$ and 1-$Pt(H_2O)Cl$ hydrolysis products. In this case the absence of Ph groups is felt and the planar structures tend to become tetrahedral. The behavior of the >d,l form, however, is not clear.

Comparison between the reactants and products

Table 5 list the variation of some parameters accompanying the first hydrolysis reaction. It is readily seen that:

(i) The difference in the orbital stabilization energy, ΔEH is always negative, which shows that the hydrolysis reaction should be exothermic, apart from $Pt(NH_3)_2Cl_2$, the largest gain in energy is obtained for 3-$PtCl_2$, ¦d,l form. This form has the second best ΔMM and the best ΔSE, although both ΔMM and ΔSE vary only slightly.

(ii) The variation of Δq(Pt) are insignificant, apart from the fact that they are both positive which means lower negative charge on Cl and high positive charge on Pt after hydrolysis. These two changes make the substitution of the second Cl less probable, compared with the substitution of the first Cl by a water molecule. The same results were obtained for *cis*-$Pt(NH_3)_2Cl_2$ and *cis*-$(NH_3)_2Cl(H_2O)^+$ in the literature [25a–c].

Conclusions

(1) The chair and gauche conformers of the coordinated substituted en ligands differ considerably and there is a marked preference for the gauche isomer. In the case of 1-$PtCl_2$ the conformation of the substituted en affects the bond parameters and could be essential in provoking the release of one Cl^- after the uptake of a water molecule in the S_N2-governed aquation reaction.

(2) The presence of the OH substituents in the phenyl rings is essential for 3-$PtCl_2$ (OH are in 2-position) behavior. The *meso* isomer of this compound showed slower hydrolysis then the $>d,l$ isomer due to the 5th contact between the O atom from the OH group and the Pt atom, which is almost perpendicular to the best PtN_2Cl_2 plane. This contact hinders the entrance of a water molecule and the formation of the transition state complex and thus makes hydrolysis much slower. In the $>d,l$ isomer of this compound both phenyl substituents are in equatorial positions and such a 5th contact is not possible.

(3) The bulkier ligands contribute additionally to stabilizing the Pt(II) compounds in a planar coordination. Since these compounds with bulkier ligands are exactly those that show greater Cl^- lability and higher cytostatic effects, it may be concluded that the hydrolysis reaction does not involve planar–tetrahedral conversion. The bulkier ligands also tend to stabilize the mono aquo complex thus contributing to the energy of formation of this complex. It appears that a correlation exists between the thermodynamic stability and the rate of hydrolysis – the more stable compounds hydrolyze faster, but the entropy factor as displayed by the difference in the behavior of the isomer forms of 3-$PtCl_2$ should not be ignored.

Acknowledgements

N.T. is grateful to the University of Regensburg (Germany) and the German Science Foundation (DFG) for providing financial support during her stay in Germany. Financial support by the Bulgarian National Research Fund through Grants 136 and 306 is also acknowledged. The authors are grateful to Dr Weniger and Dr Homeier from the University of Regensburg (Germany) for critically reading the manuscript.

References

1 C.A. Lepre and S.J. Lippard, in F. Eckenstein and D.M.J. Lilley (eds.), *Nuclei Acids and Molecular Biology,* Vol. 4, Springer, Berlin, 1990.
2 B. Lippert, *Prog. Inorg. Chem., 37* (1989) 2; P. Umapathy, *Coord. Chem. Rev., 95* (1989) 129.
3 B. Rosenberg, L. Van Camp and T. Krigas, *Nature (London), 205* (1965) 698.
4 B. Wappes, M. Jennerwein, E.V. Angerer, H. Schönenberger, J. Engel, M. Berger and K.-H. Wrobel, *J. Med Chem., 27* (1984) 1280.
5 R. Muller, R. Gust, G. Bernhard, C. Keller, H. Schonenberger, S. Seeber, R. Osieka, A. Eastman and M. Jennerwein, *J. Cancer Res. Clin. Oncol., 116* (1990) 237.
6 (A) G. Bernhardt, R. Gust, H. Reile, H.-D. v. Orde, R. Muller, C. Keller, T. Spruss, H. Schönenberger, T. Burgermeister, A. Mannschreck, K.-J. Range and U. Klement, *J. Cancer Res. Clin. Oncol., 118* (1992) 201; (b) M. Jennerwein, B. Wappes, R. Gust, H. Schönenberger, J. Engel, S. Seeber and R. Osieka, *J. Cancer Res. Clin. Oncol., 114* (1988) 347.
7 M. Jennerwein, R. Gust, R. Müller, H. Schönenberger, J. Engel, M.R. Berger, D. Schmähl, S. Seeber, R. Osieka, G. Atassi and D.M.-De Bock, *Arch. Pharm. (Weinheim), 322* (1989) 67.
8 D.P. Bancroft, C.A. Lepre and S.J. Lippard, *J. Am. Chem. Soc., 112* (1990) 6860.
9 S.E. Miller, K.J. Gerard and A. Hause, *Inorg. Chim. Acta, 190* (1991) 135.
10 T.W. Hambley, *Inorg. Chem., 30* (1991) 937.
11 F.A. Cotton and G. Wilkinson, *Advanced Inorganic Chemistry,* Interscience, New York, 3rd edn., 1972.
12 J. Demuynck, A. Veillard and U. Wahlgren, *J. Am. Chem. Soc, 95* (1973) 5563.
13 D.L. Kepert, *Prog. Inorg. Chem., 24* (1978) 180.
14 (a) J.C. Bailar, Jr., *Coord. Chem. Rev., 100* (1990) 1; (b) T.A. Albright, J.K. Burgett and M.-H. Whangho, *Orbital Interactions in Chemistry,* Wiley, New York, 1985, pp. 305–309.
15 J. Iball, M. McDougall and S. Scrimgeour, *Acta Crystallogr., Sect. B, 31* (1975) 1672.
16 G.H.W. Milburn and M.R. Truter, *J. Chem. Soc. A,* (1966) 1609.
17 H.E. Howard-Lock, C.J.L. Lock, G. Turner and M. Zvagulis, *Can. J. Chem., 59* (1981) 2737.
18 C.J.L. Lock and M. Zvagulis, *Inorg. Chem., 20* (1981) 1817.
19 R.H.B. Mais, P.G. Owston and A.M. Wood, *Acta Crystallogr, Sect. B, 28* (1972) 393.
20 G. Zanotti, A.D. Pra, G. Bombieri and A.M. Tamburro, *Acta Crystallogr., Sect. B, 34* (1978) 2138.
21 A.T. Baker and M.T. Emett, *Aust. J. Chem., 45* (1992) 429.
22 H. Basch, M. Krauss, W.J. Stevens and D. Cohen, *Inorg. Chem., 24* (1985) 3313.
23 M.-B. Krogh-Jespens and A. Attonen, *Inorg. Chem, 26* (1987) 2048.
24 J Lipinski, *Inorg. Chim. Acta, 152* (1988) 151.
25 (a) A.A. Tulub, *Zh. Neorg. Khim., 37* (1992) 1332; (b) A.S. Dimoglo, Yu. M. Chumakov and I.B. Bersuker, *Teor. Eksp. Khim., 16* (1980) 668; *17* (1981) 88; (c) A.S. Dimoglo, Yu. M. Chumakov and I.B. Bersuker, *Koord. Khim., 12* (1980) 1879.
26 B.D. El-Issa, M.A. Makhyoun and B.A. Salsa, *Inst. J. Quantum Chem., 31* (1987) 295.
27 MMX, *QCPE 395,* Bloomington, IN, USA.
28 G. Calzaferri, L. Forss and I. Kamber, *J. Phys. Chem., 93* (1989) 5366.
29 N.J. Fitzpatrick and G.H. Murphy, *Inorg. Chim. Acta, 111* (1986) 139; *87* (1984) 41.
30 (a) R. Jostes, *Theor. Chim. Acta, 74* (1988) 229; (b) V.I. Baranovskii and A.V. Nikol'skii, *Teor. Eksp. Khim., 3* (1967) 527.
31 P.G. Abdul-Ahad and G.A. Webb, *Int J Quantum Chem., 21* (1982) 1105.
32 (a) A.S. Dimoglo, N. Czoban, Yu. M. Chumakov and I.B. Bersuker, *Khim.-Farm. Zh., 60* (1980); (b) J.B. Goddard and F. Basolo, *Inorg. Chem., 7* (1968) 936, and refs. therein.
33 R. Muller, R. Gust, G. Bernhardt, Ch. Keller, H. Schönenberger, S. Seeber, R. Osieka, A. Eastman and M. Jennerwein, *J. Cancer Res Clin Oncol., 116* (1990) 237.
34 R. Gust, H. Schonenberger, J. Kritzenberger, U. Klement and K.-J. Range, *Inorg. Chim. Acta,* to be published.

Appendix

The EH parameters used in the present study are:

H	$\xi(1s) = 1.300$,	$H_{ss} = -13.60$ eV
C	$\xi(2s) = 1.725$,	$H_{ss} = -21.40$ eV
	$\xi(2p) = 1.625$,	$H_{pp} = -11.40$ eV
N	$\xi(2s) = 1.950$,	$H_{ss} = -26.00$ eV
	$\xi(2p) = 1.950$,	$H_{pp} = -13.40$ eV
O	$\xi(2s) = 2.275$,	$H_{ss} = -32.30$ eV
	$\xi(2p) = 2.275$,	$H_{pp} = -14.80$ eV
Cl	$\xi(3s) = 2.183$,	$H_{ss} = -26.30$ eV
	$\xi(3p) = 1.733$,	$H_{pp} = -14.20$ eV
Pt	$\xi(6s) = 2.940$,	$H_{ss} = -9.08$ eV
	$\xi(6p) = 2.940$,	$H_{pp} = -5.48$ eV
	$\xi_1(5d) = 4.084$,	$H_{dd} = -12.59$ eV $\quad c_1 = 0.798$
	$\xi_2(5d) = 1.840$	$c_2 = 0.352$

The Pt(II) valence state ionization potentials (in eV) are [31]:

	A	B	C
$d(d^n)$	0.775	11.014	8.566
$d(d^{n-1}s)$	0.434	12.198	11.157
$d(d^{n-1}p)$	0.434	12.421	12.148
$s(d^{n-1}s)$	0.403	8.324	8.715
$s(d^{n-1}s^2)$	−0.099	9.582	10.004
$s(d^{n-2}sp)$	0.062	8.615	11.268
$p(d^{n-1}p)$	0.465	6.799	4.475
$p(d^{n-2}p^2)$	1.035	6.378	5.492
$p(d^{n-2}sp)$	1.035	6.378	5.492